Braz J Phys (2017) 47:426–435
DOI 10.1007/s13538-017-0515-y

PARTICLES AND FIELDS

Maximum Entropy Inferences on the Axion Mass in Models with Axion-Neutrino Interaction

Alexandre Alves[1] · Alex Gomes Dias[2] · Roberto da Silva[3]

Received: 14 April 2017 / Published online: 7 July 2017

Abstract In this work, we use the maximum entropy principle (MEP) to infer the mass of an axion which interacts to photons and neutrinos in an effective low energy theory. The Shannon entropy function to be maximized is defined in terms of the axion branching ratios. We show that MEP strongly constrains the axion mass taking into account the current experimental bounds on the neutrinos masses. Assuming that the axion is massive enough to decay into all the three neutrinos and that MEP fixes all the free parameters of the model, the inferred axion mass is in the interval $0.1\ \text{eV} < m_A < 0.2\ \text{eV}$, which can be tested by forthcoming experiments such as IAXO. However, even in the case where MEP fixes just the axion mass and no other parameter, we found that $0.1\ \text{eV} < m_A < 6.3\ \text{eV}$ in the DFSZ model with right-handed neutrinos. Moreover, a light axion, allowed to decay to photons and the lightest neutrino only, is determined by MEP as a viable dark matter candidate.

Keywords Maximum entropy principle · Axion-neutrino interaction · Dark matter

✉ Roberto da Silva
rdasilva@if.ufrgs.br

[1] Departamento de Física, Universidade Federal de São Paulo, UNIFESP, Diadema, Brazil

[2] Centro de Ciências Naturais e Humanas, Universidade Federal do ABC, UFABC, Santo André SP, 09210-170, Brazil

[3] Instituto de Física, Universidade Federal do Rio Grande do Sul, UFRGS, Porto Alegre RS, 91501-970, Brazil

1 Introduction

Although the discovery of the Higgs boson and its properties have represented a major advance for verifying the mass generation mechanism through spontaneous symmetry breaking, along with its consequences, an explanation for the values of most of the elementary particles masses is still missing. It is understood in the standard model (SM) that the photon has zero mass due to an unbroken gauge symmetry, and the weak vector bosons W and Z^0 have interdependent masses resulting from the electroweak symmetry breakdown. Still, according to the Standard Model, the Higgs boson and all the charged fermions have arbitrary nonzero masses, with the neutrinos being massless. This last feature is in contradiction with the neutrinos oscillation phenomena, whose description requires nonzero neutrino mass differences. As a matter of fact, the present experimental limits show that neutrinos are ultralight compared to the other known massive particles. All of this might suggest that a new principle or mechanism is necessary to reach a more satisfactory understanding of the elementary particles masses.

It was found in ref. [1] that the peak of a function constructed by multiplying the basic fourteen Standard Model branching ratios of the Higgs boson decay channels occurs for a Higgs boson mass which is in good agreement with the experimental value measured at the LHC [2]. Additionally, it was also mentioned in ref. [1] a possible analogy with some sort of entropy arguing that the mass of the Higgs boson has a value that allows for the largest number of ways of decays into elementary particles. The work of ref. [3] indeed showed that the value of the Higgs boson mass results from the maximum entropy principle (MEP) [4–6],

where the information entropy is suitably defined in terms of the Higgs branching ratios into Standard Model particles, furnishing the most accurate theoretical Higgs boson mass determination to date.

Our premise in invoking MEP is to consider an ensemble of N non-interacting identical spinless particles which have m basic decay modes. The probability that the ensemble evolves to a final state configuration, with n_0 bosons decaying into the mode with branching ratio BR_0, n_1 bosons decaying into the mode with branching ratio BR_1, and so on until n_m bosons decaying into the mode having branching ratio BR_m, is given by the following multinomial distribution

$$\Pr(\{n_k\}_{k=0}^m) \equiv \frac{N!}{n_0!n_1!\cdots n_m!}\prod_{k=0}^{m}(BR_k)^{n_k}, \tag{1}$$

in which $\sum_{k=0}^m BR_k = 1$, and $\sum_{k=0}^m n_k = N$. From these probabilities, the Shannon entropy [7] associated to the evolution of the initial ensemble to the final state in which all N scalars have decayed is given by

$$S_N = -\sum_{\{n_i\}}^{N}\Pr(\{n_k\}_{k=0}^m)\ln\Pr(\{n_k\}_{k=0}^m)\,, \tag{2}$$

with $\sum_{\{n_i\}}^N(\bullet) \equiv \sum_{n_0=0}^N\sum_{n_1=0}^N\cdots\sum_{n_m=0}^N(\bullet)\times\delta\left(N-\sum_{i=0}^m n_i\right)$ [3]. The entropy S_N is a function of unknown quantities as masses of particles and coupling constants entering in the branching ratios BR_k. We propose that such quantities can be inferred through maximization of S_N, also taking into account constraints that may enter as prior information. Similar approaches using information and configurational entropies can be found, for example, in refs. [8–13].

Our aim in this work is to use MEP to infer the mass of the axion, taking into account a model in which the axion decays to neutrinos and photons. More specifically, we made the following assumptions on the axion field, $A(x)$. First, its particle excitation, the axion, decays dominantly into a pair photons and also into a pair of neutrinos. Second, its low energy effective Lagrangian describing the interactions with photons and neutrinos is given by

$$\begin{aligned}\mathscr{L}_{eff} = \frac{1}{2}\partial_\mu A\,\partial^\mu A - \frac{1}{2}m_A^2\,A^2 - \frac{g_{A\gamma}}{4}\,A\,F_{\mu\nu}\widetilde{F}^{\mu\nu}\\ - \frac{g_{A\nu}}{2}\,\overline{\nu}_i\gamma^\mu\gamma_5\nu_i\,\partial_\mu A\end{aligned} \tag{3}$$

where $F^{\mu\nu}$ is the electromagnetic field strength with $\widetilde{F}^{\mu\nu} \equiv \epsilon^{\mu\nu\lambda\rho}F_{\lambda\rho}/2$ its dual; $\nu_i(x)$, $i = 1, 2, 3$, denote the mass eigenstates neutrinos fields; m_A is the axion mass; f_A the axion decay constant, which is a high energy scale; and $g_{A\gamma}$ and $g_{A\nu}$ are the axion-photon and axion-neutrino coupling constants, respectively. Another important remark is that we are tacitly assuming that neutrinos are Dirac fermions. Therefore, the coupling between the axion and the neutrinos vanish in the massless limit. In the Appendix A, we show an example of an ultraviolet completed model leading to the effective Lagrangian in (3).

The axion is a hypothetical pseudo Nambu-Goldstone boson remnant of an anomalous $U(1)$ symmetry, spontaneously broken at the energy scale f_A, present in extensions of the Standard Model motivated to solve the strong CP problem through the Peccei-Quinn mechanism [14–16] (for a review of the strong CP problem and axions, see, for example, refs. [17, 18]). Experiments searching for the axion constrain f_A to be much above the electroweak scale, i.e., $f_A \gg v = 246$ GeV. Consequently, the axion interacts very weakly with all other particles by the reason that the associated coupling constants are suppressed by f_A. We define the axion-neutrino coupling constant in (3) as

$$g_{A\nu} = \frac{C_{A\nu}}{f_A}, \tag{4}$$

where $C_{A\nu}$ is the coefficient of the axion-neutrino coupling which depends on the ratios of vacuum expectation values (see Appendix A). The axion-photon coupling constant is, by its turn,

$$g_{A\gamma} = \frac{\alpha}{2\pi f_A}\widetilde{C}_{A\gamma}\,, \tag{5}$$

with α the fine structure constant, and the coefficient of the axion-photon coupling

$$\widetilde{C}_{A\gamma} = \left(\frac{C_{a'\gamma}}{C_{a'g}} - \frac{2}{3}\frac{4+m_u/m_d}{1+m_u/m_d}\right). \tag{6}$$

In the coefficient $\widetilde{C}_{A\gamma}$ the anomaly coefficients $C_{a'\gamma}$ and $C_{a'g}$ are model dependent and typically of order one, with $m_u/m_d \approx 0.56$ the ratio of up and down quark masses. Such coefficients for different models, as well as other features of the axion, can be found in [19]. Additionally, the axion mass is also suppressed by the energy scale f_A and given by [15]

$$m_A \simeq \frac{m_\pi f_\pi}{f_A}\frac{\sqrt{m_u/m_d}}{1+m_u/m_d} \approx 0.48\frac{m_\pi f_\pi}{f_A}, \tag{7}$$

in which m_π and f_π are the pion mass and its decay constant, respectively. This makes the axion an ultralight particle for $f_A \gg 246$ GeV.

Our paper is organized as follows: In the next section, we briefly discuss how we intend to use the MEP in order to obtain the axion mass considering the lightest neutrino mass and the coupling constants as inputs. In Section 3, we present a first part of our results which consider axions decaying into pairs of neutrinos and pair of photons, and a second part of the results corresponding to axions decaying only into pair of the lightest neutrinos, in addition to a pair of photons, which is presented in Section 4. We present our conclusions in Section 5.

2 Parameters Inferences from MEP

Let us consider an initial state ensemble with a very large number N of axions. After a time $t \gg 1/\Gamma$, with the total axion decay width given by the sum of the partial decay widths into a pair of photons, Γ_0, plus the ones into pairs of neutrinos, Γ_i, i. e.,

$$\Gamma = \Gamma_0 + \sum_i \Gamma_i \ , \tag{8}$$

the initial state ensemble evolves to a final state bath of photons and neutrinos. The summation above (and below) extends only over those neutrinos whose masses are less than $m_A/2$. If the axion is massive enough, it could decay in all the three active neutrinos, where $i = 1,\ 2,\ 3$.

The axion partial decay widths derived from the effective Lagrangian in (3) are

$$\Gamma_0 \ = \ \frac{g_{A\gamma}^2}{64\pi} m_A^3 \ , \tag{9}$$

$$\Gamma_i \ = \ \frac{g_{A\nu}^2}{8\pi} m_A m_i^2 \beta_i \ , \tag{10}$$

where m_i is the ith neutrino mass and $\beta_i = \sqrt{1 - \frac{4m_i^2}{m_A^2}}$.

These widths lead to the following branching ratios for the axion decaying into a pair of photons and into pairs of neutrinos

$$BR_0 \ = \ \frac{\Gamma_0}{\Gamma} = \left[1 + \sum_i 32\pi^2 \frac{r_\nu^2}{\alpha^2} \frac{m_i^2 \beta_i}{m_A^2} \right]^{-1} \ , \tag{11}$$

$$BR_i \ = \ \frac{\Gamma_i}{\Gamma} = \left[1 + \frac{\alpha^2}{32\pi^2 r_\nu^2} \frac{m_A^2}{m_i^2 \beta_i} + \sum_{j \neq i} \frac{m_j^2 \beta_j}{m_i^2 \beta_i} \right]^{-1} \ , \tag{12}$$

in which we define $r_\nu \ = \ \left| C_{A\nu} / \widetilde{C}_{a\gamma} \right|$ as the ratio of the anomaly coefficients of the axion-neutrino coupling, $C_{A\nu}$, and the axion-photon coupling, $\widetilde{C}_{A\gamma}$. This ratio is equivalent to the ratio of the associated coupling constants given by $\left| g_{A\nu} / g_{A\gamma} \right| = 2\pi r_\nu / \alpha$.

There are many possible final states characterized by the number of axions which decay into a pair of photons, n_0, and by the numbers axions which decay into each possible pair of neutrinos, n_i, $i = 1, 2, 3$. Considering that the axion can decay into the three neutrinos plus the photon, according to (1), the probability that the ensemble of N axions decay into a particular final state characterized by n_0, n_1, n_2, and n_3 is

$$\Pr(\{n_k\}_{k=0}^3) = \frac{N!}{n_0! n_1! n_2! n_3!} \prod_{k=0}^{3} (BR_k)^{n_k} \ . \tag{13}$$

The entropy function is then constructed from (2) summing over all the partitions satisfying $\sum_{k=0}^3 n_k = N$.

According to MEP, the initial ensemble evolves to a final state of maximum entropy permitting us to infer the values of the unknown quantities through maximization of S_N. We do this by taking into account the prior information of the neutrinos masses from the best fit mass squared differences determined by the data of neutrinos oscillations, considering the normal hierarchy pattern [20],

$$\begin{aligned} \Delta m_{12}^2 \ &= \ m_2^2 - m_1^2 = (7.45 \pm 0.25) \times 10^{-5}\, \mathrm{eV}^2 \\ \Delta m_{31}^2 \ &= \ m_3^2 - m_1^2 = (2.55 \pm 0.05) \times 10^{-3}\, \mathrm{eV}^2 . \end{aligned} \tag{14}$$

Thus, S_N depends, effectively, on the three parameters m_A, r_ν, and the lightest neutrino mass which we denote as m_ν. Finally, our analysis do not depend on the neutrinos mass hierarchy pattern, the same results are obtained if the inverted hierarchy is assumed.

Contrary to the situation of the Higgs boson mass inference carried out in ref. [3], where the Higgs mass was the last independent Standard Model parameter to be determined, in the model under study we have three independent parameters as we just discussed. In principle, MEP could force all these parameters to be fixed at the global maximum of the entropy. However, this is not the case of the Standard Model, for example. The Higgs mass does not correspond to a global maximum of S, but just to a constrained maximum. Some parameters of the Standard Model are related by its symmetries imposing strong constraints on these parameters, for example, the W and Z bosons masses. This fact reveals that not all the parameters of the model might be determined by the MEP. Nevertheless, the success in the Higgs mass prediction suggests that MEP can be useful in inferring the masses of scalar particles when the other parameters are fixed by some different mechanism.

In this work, we remain agnostic about the type of inference that MEP can actually perform, waiting for the experimental evidence to settle that. Therefore, we take two main hypothesis: first, the entropy function is maximized in m_A only, with the other parameters considered as prior information, that is, $S_N \equiv S_N(m_A | m_\nu, r_\nu)$; second, a more restrict hypothesis: $S_N \equiv S_N(m_A, m_\nu, r_\nu)$ where we will show that MEP can be more determinant in the sense that having information about one of the parameters: (i) axion mass, (ii) neutrino mass, and (iii) ratio of the coupling constants, the other two parameters can be uniquely determined by this principle.

The ratio r_ν and the lightest neutrino mass m_ν are free parameters which should be determined prior to the inference of axion mass. However, it is important to mention that the Shannon entropy in our formulation is not defined as a entropy per particle, a function of an energy per particle, as is usual in Thermodynamics. This does not represent

a problem, however. First of all, our weights in Shannon entropy are not Boltzmann weights of some known problem of interacting particles in contact with a thermal reservatory exactly as is studied in Statistical Mechanics. Only in this situation, the Shannon entropy should be equivalent to Boltzmann entropy definition. Nevertheless, even without this equivalence it is important to mention that MEP is a more general and universal method than the Statistical Mechanics approach, and its basis are governed by probability theory. In this context, we can write the entropy of any probability distribution and maximize it in relation to their physical parameters.

We impose the most recent experimental constraints from the neutrino oscillation experiments summarized in ref. [20]

$$m_1 = m_\nu \ , \quad m_2 = \sqrt{m_\nu^2 + 7.45 \times 10^{-5}}$$
$$m_3 = \sqrt{m_\nu^2 + 2.55 \times 10^{-3}} \ . \tag{15}$$

The upper bound from the Planck Collaboration measurements of CMB anisotropies [21] for the sum of the neutrino masses, along with (15) for a massless lightest neutrino, translate to the following constraint that will be taken into account in our inference process

$$0.059 \text{ eV} < \sum_{i=1}^{3} m_i < 0.23 \text{ eV}, \tag{16}$$

which implies the interval $0 < m_\nu < 0.0712$ eV, for the lighest neutrino mass. In the next sections we will present our results.

3 Results I: Axions Decaying into the Three Neutrinos and Photons

First, we suppose that the axion is heavy enough to decay into a pair of photons and all the three neutrinos.

The entropy, given by (2), can be written as [22]

$$S_N(m_A|m_\nu, r_\nu) = S(m_A|m_\nu, r_\nu) + \frac{3}{2}\ln(2\pi Ne) + O\left(\frac{1}{N}\right) \tag{17}$$

with

$$S(m_A|m_\nu, r_\nu) = \frac{1}{2}\ln(BR_0 BR_1 BR_2 BR_3) \tag{18}$$

where the branching ratios are related as $\sum_{i=0}^{3} BR_i = 1$.

It can be shown that the global maximum of S is obtained when all the branching ratios are equal

$$BR_i(m_A, m_\nu, r_\nu) = \frac{1}{4} \ , \ i = 0, 1, 2, 3 \tag{19}$$

However, it is also possible that this type of solution cannot be attainable if further constraints arise from an UV complete theory in which the parameters do not allow that the (19) be satisfied. If further constraints are absent or if they are weak, then we should expect that nearly equal branching ratios constitute another prediction coming from MEP.

First of all, we investigate the entropy supposing that MEP fixes just the axion mass, i.e., $S = S(m_A|m_\nu, r_\nu)$, with the other parameters either previously known or at least bounded by some data. As we have just discussed, this might be the case if the UV complete theory fixes somehow the r_ν of the model and possibly other parameters. In our approach, we, therefore, allow m_ν to vary according to the constraints of (15), (16). In this case, for each fixed m_ν and r_ν, we just seek for a solution (m_A) that maximizes $S(m_A|m_\nu, r_\nu)$ given by (18). The light green shaded area of Fig. 1 shows the MEP inference for the axion mass for the range of the r_ν taking into account the neutrino masses constraints from (16).

The gray curves in Fig. 1 correspond to axion mass maximizing the entropy for the case in which the maximum lightest neutrino mass (upper curve) and the minimum lightest neutrino mass (lower curve) were assumed. Such curves can be identified as iso-lightest-neutrino-mass curves in the diagram $r_\nu \times m_A$. The following plots (a) and (b), in Fig. 2

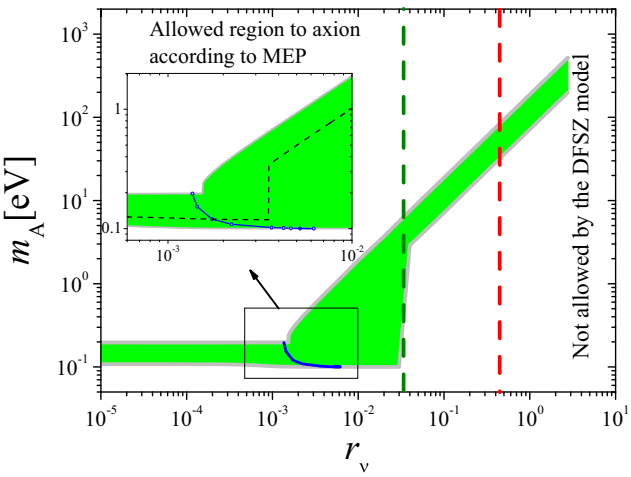

Fig. 1 Inferred axion mass region from MEP, taking into account the constraints from (16). The *gray curves* correspond to the axion mass maximizing the entropy for the case in which the maximum lightest neutrino mass (*upper curve*) and the minimum lightest neutrino mass (*lower curve*) are assumed. The *light green shaded region* correspond to all the maximum entropy points, assuming that the lightest neutrino mass is in the interval allowed by 16. The *blue curve* assumes that the maximum of entropy fixes all the three parameters as discussed in text. The *inset* plot corresponds to a zoom of the *blue line*, where the *dashed curve* is just an example of curve in the allowed region corresponding to an intermediate value of lightest neutrino mass: $m_\nu = 0.03$ eV between the bounds. This curve crosses the *blue line* in $(r_\nu, m_A) \equiv (0.00174, 0.12)$, which is the point of the highest entropy in this dashed line. Finally, the *dashed red line* shows the limit of acceptable values of r_ν for the DFSZ-type model which we present in the Appendix (A), while the *dashed dark green line* shows the limit from astrophysics for the r_ν (see the text)

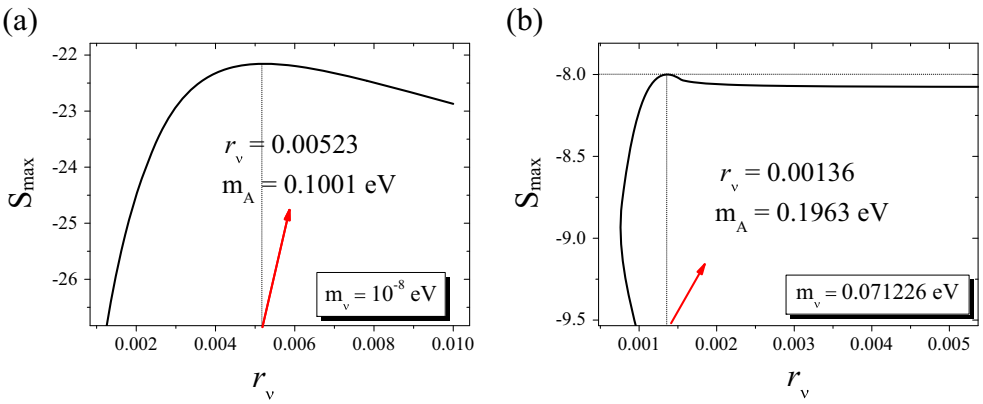

Fig. 2 The following plots (**a**) and (**b**) show the maximum entropy values assumed in each point of the *gray lines* (see Fig. 1) respectively for the minimum ($m_\nu = 10^{-8}$ eV) and the maximum ($m_\nu = 0.0721226$ eV) lightest neutrino mass. Both *gray lines* cross the *blue line* (see again Fig. 1) exactly in the points that correspond to the peak presented in the plots (**a**) and (**b**)

show the maximum entropy values assumed in each point of gray lines respectively for the minimum ($m_\nu = 10^{-8}$ eV) and the maximum ($m_\nu = 0.0721226$ eV) lightest neutrino mass. It is important to mention that even when we used $m_\nu = 10^{-7}$ eV, the same result was obtained and the gray line remains the same.

This suggests that we can look to MEP in a more restrict optimization than just seeking for a solution m_A, given m_ν and r_ν. A stronger inference can be made by optimizing $S{\equiv}S(m_A, m_\nu, r_\nu)$, the result is represented by the blue line of Fig. 2, where given one of the parameters, is possible to obtain the other two ones. We give a more detailed explanation as follows. The boundary gray lines cross the blue line exactly in the points that correspond to the peak presented in the plots (a) and (b) in the same Fig. 2. The inset plot in Fig. 1 corresponds to a focused area of the blue line region. Just to give an example, for $r_\nu = 0.00174$, the point over the blue line, of the highest entropy in the green region, corresponds to $m_A = 0.12$ eV and $m_\nu = 0.03$ eV. In this same inset plot, the dashed black curve in the allowed region corresponds exactly to the intermediate value of lightest neutrino mass: $m_\nu = 0.03$ eV. This iso-lightest-neutrino-mass curve is exactly between the limiting lines (gray lines) as expected. Therefore, the light green region can be understood as a family of iso-lightest-neutrino-mass curves of the diagram $r_\nu \times m_A$, which cross the blue line which is composed by the optimal values found in each iso-lightest-neutrino-masses curves. In other words, the blue line is composed by values for which MEP fixes all the three parameters.

The dashed red line in Fig. 1 shows the limit to allowed values of r_ν for the DFSZ-type model with right-handed neutrinos which we present in Appendix (A). In the same Fig. 1, the dashed dark green line shows the limit from astrophysics on the coupling (see below).

The inference is stronger for small r_ν up to ~ 0.0017, for higher values, the upper boundary of the Fig. 1 increases toward higher axion masses while the lower boundary remains nearly constant with r_ν. Note that, under this hypothesis, we need to know r_ν and m_ν in order to get m_A. The DFSZ model with right-handed neutrinos restricts $r_\nu < 0.46\cos^2\beta$, which determines the dashed red line (see Appendix (A)).

We observe that under the consideration of more restrict optimization (blue line in Fig. 1), MEP constrains the axion mass to lie within

$$0.1 \text{ eV} < m_A < 0.2 \text{ eV}. \tag{20}$$

We observe that the interval in (20) is in the threshold of the projected sensitivity of the IAXO experiment [23]. This shows that our hypothesis can be tested experimentally in the near future.

We should mention that the interval of (20) for the axion mass derived from MEP is compatible with the limits from astrophysics (compilation of the actual astrophysical limits on the axion mass and coupling constants are given in ref. [24]). For example, studies concerning the evolution of stars on the horizontal branching [25] put the constraint $m_A < 0.5$ eV ($f_A > 1.3 \times 10^7$ GeV) on the DFSZ model. There is an astrophysical limit that could potentially impact on the interval in (20), but it also depends on the axion-electron coupling. A bound from red giants in the Galactic globular cluster M5 provided $m_A \cos^2\beta < 15.3$ meV at 95% CL [26], in the DFSZ model having the axion-electron coupling coefficient $C_{Ae} = \cos^2\beta/3$[1]. Taking into account (20), it means that $\cos^2\beta < 0.0752$ implying that $r_\nu < 0.034$, with $C_{A\nu} = -C_{Ae}$. This restriction on r_ν is shown in Fig. 1 (dark green dashed line) which leads to $0.1 \text{ eV} < m_A < 6.3$ eV for the DFSZ model with the right-handed neutrinos which we present in Appendix (A).

[1] In the DFSZ model, this happens to be the case in which the right-handed electron field couples to the same Higgs doublet that give mass to the u-type quarks. If, on the other hand, the right-handed electron field couples to the same Higgs doublet that give mass to the d-type quarks then the axion-electron coupling coefficient turns out to be $C_{Ae} = -\sin^2\beta/3$, as can be seen in the Appendix (A), and the corresponding astrophysical limits turns out to be on $m_A \sin^2\beta$.

4 Results II: Axions Decaying into the Lightest Neutrinos and Photons

Let us suppose now that the axion has only two decay modes: one into a pair of photons, and the other into a pair of the lightest neutrinos. In this case, the two relevant branching ratios are

$$BR_0 = \left[1+32\pi^2\frac{r_\nu^2}{\alpha^2}\frac{m_\nu^2}{m_A^2}\left(1-\frac{4m_\nu^2}{m_A^2}\right)^{1/2}\right]^{-1} \quad \text{and} \quad BR_1 = 1-BR_{\gamma\gamma} \tag{21}$$

The probability of N axions decaying in n_0 photon pairs and $n_1 = N - n_0$ neutrino pairs is

$$\Pr(N; n_0) = \frac{N!}{n_0!(N-n_0)!} BR_0^{n_0}(1-BR_0)^{N-n_0} \tag{22}$$

In the limit $N \to \infty$, by the central limit theorem, $\Pr(N; n_0) \to \frac{\exp\left[-\frac{(n_0 - N\cdot BR_0)^2}{2NBR_0(1-BR_0)}\right]}{\sqrt{2\pi N\cdot BR_0(1-BR_0)}}$ and the entropy can be written as

$$S_N = S_0 + \frac{1}{2}\ln(2\pi Ne) + O\left(\frac{1}{N}\right) \tag{23}$$

$$S_0(m_A, m_\nu, r_\nu) = \frac{1}{2}\ln\left[BR_0\cdot(1-BR_0)\right] . \tag{24}$$

In this case, the maximum of S_N given by (23) occurs for

$$BR_0 = BR_1 = 1/2 , \tag{25}$$

in close analogy to 19.

In the Appendix (B), we derive the algebraic solutions to this equation in details. An important difference to the previous case is that, as shown in the Appendix (B), the solutions of (25) can only be found in terms of the ratio $z \equiv m_\nu/m_A$. This implies that one parameter remains necessarily free in the inference method. There are two interesting asymptotic regimes which we want to discuss. First $z \approx 1/2$, and second $z << 1$.

The first one is the threshold regime where $m_A \approx 2m_\nu$. This is a type of solution which we also found in the case where the Higgs boson has an additional decay channel to dark matter [3].

The second interesting regime occurs when $m_\nu << m_A$, in this case, it is possible to show that (see Appendix B)

$$\frac{m_\nu}{m_A} \approx \frac{\sqrt{1-\sqrt{1-\frac{\alpha^2}{4\pi^2 r_\nu^2}}}}{2} \tag{26}$$

Moreover, as this relation should be positive, there is a lower bound on r_ν given by

$$r_\nu = \frac{\sqrt{3\sqrt{3}}}{4\pi}\alpha = 0.00132 \tag{27}$$

which is a solution of the fourth order equation in z explicit in the Appendix B. This is compatible with the inferred couplings in the case of three neutrinos studied in the previous section.

In the Fig. 3, we show the inferred masses as a function of the axion-neutrino coupling. The upper plot in Fig. 3 displays the $z << 1$ regime. The axion and the neutrino masses can be very different depending on r_ν which varies from the smallest possible value of 0.00132, for which z is positive, up to the maximum value of 0.46 allowed by the axion model under consideration. In the lower plot, we show the other interesting regime where $m_A \approx 2m_\nu$, again allowing the range $0.00132 < r_\nu < 0.46$. In this former case, the mass inference is barely dependent of the coupling constant. In both plots, we also show the region of the axion mass parameter where the axion can constitute, at least, part of the cold dark matter of the Universe and be detected

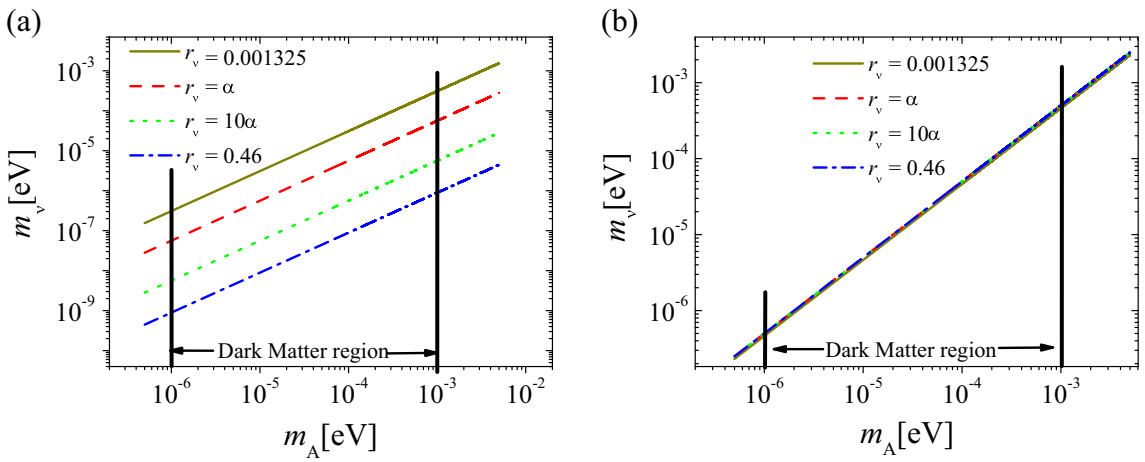

Fig. 3 Linear relations predicted by maximizing the Shannon entropy in the case where the axion is allowed to decay just to the lightest neutrino and photons. In the plot (**a**), we show the $z \approx 1/2$ regime, and in the plot (**b**), the $z << 1$ regime

by a haloscope like [27], or other proposed experiments as [28–30].

Recently, the axion mass was calculated with lattice QCD methods [31, 32] to lie in the range 10^{-6} eV$< m_A < 1.5 \times 10^{-3}$ eV which fits exactly in the bulk of the region shown inside the bars in Fig. 3. If the axion mass confirms the lattice QCD result, one can use the MEP prediction to bound the lightest neutrino mass and the coupling constant with the results presented in this work. Once confirmed, this would add a strong evidence in favor of MEP as a valuable inference tool in particle physics.

5 Conclusions

In this paper, we employed the maximum entropy principle to a model where axions couple to photons and neutrinos. By demanding that the Shannon entropy of an ensemble of axions decaying to photons and neutrinos be maximized, we made inferences about the masses of the axion taking into account its relationship with neutrinos masses and r_ν, which is proportional to the ratio of axion-neutrino coupling constant and axion-photon coupling constant.

In the case where the axion decays into the three neutrino mass eigenstates, and taking the hypothesis that the entropy is assumed to be a function of the axion mass, the lightest neutrino mass, and the r_ν which is the ratio of the axion coupling constants, MEP is able to make a sharp prediction: $0.1 \text{ eV} < m_A < 0.2$ eV. On the other hand, if r_ν and m_ν are given as inputs, i.e., $S = S(m_A|r_\nu, m_\nu)$, considering the DFSZ model with right-handed neutrinos, MEP jointly with astrophysical bounds, constrain the axion mass to be $0.1 \text{ eV} < m_A < 6.3$ eV.

If the axion decays only into a pair of the lightest neutrinos and photons, the inference has two regime of solutions allowing the axion as a dark matter candidate. First, when the axion mass is much larger than the lightest neutrino mass, ($z << 1$), the inference of the axion mass has a strong dependence on the ratio of the coupling constant (r_ν) as shown in Fig. 3a. On the other hand, if $m_A \approx 2m_\nu$ ($z \approx 1/2$), the axion mass has a very weak dependence on r_ν as expected (see Fig. (3)b). For example: if $m_A = 10^{-4}$ eV, and $z \approx 1/2$, the MEP fixes the lightest neutrino mass around 5×10^{-5} eV; However, if $z << 1$, the MEP predicts lightest neutrino mass within $10^{-8}\text{eV} < m_\nu < 10^{-5}\text{eV}$. In this case, for example, if $r_\nu = \alpha$, then $m_\nu = 7 \times 10^{-6}$ eV.

Finally, we would like to stress that MEP can furnish a sharp prediction if the neutrino mass is determined and knowing r_ν from some model as shown in our Fig. 1.

Acknowledgements This research was partially supported by the CNPq grants 307098/2014-1 (A.A.), 306636/2016-6 (A.G.D.), and 458498/2014-9, 310017/2015-7 (R.S.). The work of A.A. and A.G.D. was supported by FAPESP, under the grant 2013/22079-8.

Appendix A: Ultraviolet Model Completion for to the Axion-Neutrinos Effective Lagrangian

The effective Lagrangian in (3) might originate from UV completed models having a global chiral $U(1)_{PQ}$ Peccei-Quinn symmetry. Such a symmetry is characterized by the fact it has an anomaly in the quarks sector, leading to a mechanism for solving the strong CP problem [14]. The $U(1)_{PQ}$ symmetry is assumed to be spontaneously broken at an very high energy scale giving rise to a pseudo Nambu-Goldstone boson, the axion [15, 16].

A model leading to the effective Lagrangian in (3) must have neutrinos fields carrying charge of the $U(1)_{PQ}$ symmetry. In order to have a plausible model, we consider the DFSZ invisible axion model [33, 34], and add to it three right-handed neutrinos ν'_{iR} [2]. The DFSZ model contains a neutral singlet scalar field, $\sigma(x)$, and two Higgs doublets, $H_u(x)$, $H_d(x)$, with all these fields carrying charge of the $U(1)_{PQ}$ symmetry. The scalar potential constructed from these fields is assumed to have a non-trivial minimum with the vacuum expectation values $\langle\sigma\rangle = v_\sigma/\sqrt{2}$, breaking the $U(1)_{PQ}$ symmetry, and $\langle H_{u,d}\rangle = [0 \; v_{u,d}/\sqrt{2}]^T$, breaking the electroweak $SU(2)_L \otimes U(1)_Y$ symmetry. These vacuum expectation values satisfies $\sqrt{v_u^2 + v_d^2} = v = 246$ GeV $\ll v_\sigma$. Also, it can be seen that the decay constant is such that $f_{a'} = \sqrt{v_\sigma^2 + 4v_u^2 v_d^2/v^2} \approx v_\sigma$.

Let us see how the coefficient $C_{A\nu}$ of the axion-neutrinos coupling in (3) are determined in a specific model. Such a coefficient depends on how the neutrinos fields couple to the scalar fields. Omitting the Goldstone bosons degrees of freedom—absorbed by the electroweak gauge bosons—σ and the neutral components of H_u, H_d can be parametrized as

$$\begin{aligned}
\sigma(x) &= \frac{v_\sigma + \rho(x)}{\sqrt{2}} \exp\left[i\frac{a'(x)}{f_{a'}}\right], \\
H_u^0(x) &= \frac{v_u + h_u(x)}{\sqrt{2}} \exp\left[-iX_u\frac{a'(x)}{f_{a'}}\right], \\
H_d^0(x) &= \frac{v_d + h_d(x)}{\sqrt{2}} \exp\left[iX_d\frac{a'(x)}{f_{a'}}\right].
\end{aligned} \tag{28}$$

[2] Recently, some axion models with right-handed neutrinos have been proposed to deal with others problems left open by the Standard Model, like, for example, the neutrinos masses, invoking the type-I seesaw mechanism [19, 35–37]. In the model example we assume here the neutrinos are taken to be of the Dirac type. Also, we do not specify any mechanism for generating small masses for those particles since this is not the focus of our work.

In this parametrization, $h_d(x)$, $h_u(x)$, and $\rho(x)$ are CP even Higgs fields, which are decoupled from the axion low energy effective Lagrangian in (3), and $a'(x)$ the CP odd pseudo-Nambu-Goldstone boson to be identified with the axion field $A(x)$. Such an identification is done by mean of the axion-gluons coupling defined as

$$\mathscr{L} \supset -\frac{\alpha_s}{8\pi}\frac{A}{f_A}G^a_{\mu\nu}\tilde{G}^{a,\mu\nu}. \tag{29}$$

so that the relation in the relation

$$\frac{A(x)}{f_A} = C_{a'g}\frac{a'(x)}{f_{a'}} \tag{30}$$

the energy scale f_A is the axion decay constant, with $C_{a'g}$ being the axion-gluon anomaly coefficient of the model. For the model, we are taking into account the axion-gluon anomaly coefficient is $C_{a'g} = 3(X_u + X_d) = 6$. The charges of the $U(1)_{PQ}$ symmetry of the scalar fields σ, H_u, and H_d are, respectively, $X_\sigma = 1$, $-X_u = -2\cos^2\beta$, and $X_d = 2\sin^2\beta$, with $\tan\beta = v_u/v_d$.

We assume that the axion-neutrino coupling arises from an interaction involving the Standard Model left-handed lepton doublets, L_i, according to the following Yukawa interaction

$$\mathscr{L} \supset F_{ij}\,\overline{L}_i\widetilde{H}_b\nu'_{jR} + h.c. \tag{31}$$

in which F_{ij}, with $i, j = 1, 2, 3$, is a 3×3 matrix, and $b = u$ or d if ν'_{iR} couples to H_u or H_u. We also assume that Majorana mass terms $m_{ij}\,\overline{\nu'^c_{iR}}\nu'_{jR}$ are suppressed, by the $U(1)_{PQ}$ symmetry or some other extra symmetry, relative to the Dirac mass terms arising from (31). Neutrinos masses at the sub-eV scale require small couplings F_{ij} ($\lesssim 10^{-12}$ for $v_d \sim 100$ GeV). It is not essential to our developments to make explicit a mechanism for achieving those small couplings F_{ij} and forbidden the Majorana mass terms, but we mention that this could be done with discrete symmetries allowing certain non-renormalizable operators [38]. After electroweak symmetry breakdown (31) leads to

$$\mathscr{L} \supset F_{ij}\frac{v_b}{\sqrt{2}}\overline{\nu}'_{iL}\nu'_{jR}\exp\left[-iX_{H_b}\frac{a'(x)}{f_{a'}}\right] + h.c. \tag{32}$$

With a chiral rotation $\nu'_{jR} \to \nu'_{jR}\exp\left[iX_{H_b}a'(x)/f_{a'}\right]$, the field $a'(x)$ is removed from the above interaction leaving it as a Dirac mass term. But the coupling of the $a'(x)$ field with the neutrinos fields is induced from the kinetic term $\overline{\nu}'_{iR}i\gamma^\mu\nu'_{iR}\partial_\mu a'$ as

$$\mathscr{L} \supset -\frac{X_{H_b}/C_{a'g}}{2f_A}\overline{\nu}_i i\gamma^\mu\gamma_5\nu_i\partial_\mu A \tag{33}$$

where ν_i denotes neutrinos mass eigenstates. Thus, defining $C_{A\nu} = X_{H_b}/C_{a'g}$ in (33) we have the axion-neutrino interaction in the effective Lagrangian of (3). The coefficient C_ν in this model is

$$C_{A\nu} = \begin{cases} -\frac{X_u}{C_{a'g}} = -\frac{\cos^2\beta}{3}, & \text{if } H_u \text{couples to } \nu'_{jR}\,, \\ \frac{X_d}{C_{a'g}} = \frac{\sin^2\beta}{3}, & \text{if } H_d \text{couples to } \nu'_{jR}. \end{cases} \tag{34}$$

For example, if only H_d couples to the charged right-handed charged leptons fields the ratio of anomaly coefficients in (6) is $C_{a'\chi}/C_{a'g} = 8/3$, so that $\widetilde{C}_{A\gamma} \approx 0.72$. In this case, $r_\nu = |C_{A\nu}/C_{A\gamma}| \approx 0.46\cos^2\beta$ (or $0.46\sin^2\beta$). On the other hand, if only H_u couples to the charged right-handed charged leptons fields the ratio of anomaly coefficients in (6) is $C_{a'\gamma}/C_{a'g} = 2/3$, and $\widetilde{C}_{A\gamma} \approx -1.28$. In this case, $|r_\nu| = |C_{A\nu}/C_{A\gamma}| \approx 0.26\cos^2\beta$ (or $0.26\sin^2\beta$). The expressions for the coefficients $C_{a'\gamma}/C_{a'g}$ can be found in [19].

Just for completion, we present the axion-electron coupling in the DFSZ model we are considering. Proceeding with a chiral rotation in the right-handed charged leptons singlet fields $e'_{iR} \to e'_{iR}\exp\left[-iX_{H_b}a'(x)/f_{a'}\right]$ the coefficients of the axion-electron derivative coupling is

$$C_{Ae} = \begin{cases} \frac{X_u}{C_{a'g}} = \frac{\cos^2\beta}{3}, & \text{if } H_u \text{couples to } e'_{iR}\,, \\ -\frac{X_d}{C_{a'g}} = -\frac{\sin^2\beta}{3}, & \text{if } H_d couples to e'_{iR}. \end{cases} \tag{35}$$

Appendix B: Algebraic Solutions in the One Neutrino Case

The solution of this equation $BR_{\gamma\gamma}(C_\nu, m_A, m_\nu) = 1/2$ leads to the equation

$$G(z) = z^2(1-4z^2)^{1/2} = \alpha^2/(32\pi^2 r_\nu^2) \tag{36}$$

where $z^2 = \frac{m_\nu^2}{m_A^2}$. Writing such equation in $x = z^2$, a simple cubic equation appears:

$$ax^3 + bx^2 + cx + d(r_\nu) = 0 \tag{37}$$

where $a = 4$, $b = -1$, $c = 0$ and, $d(r_\nu) = \left(32\pi^2\frac{r_\nu^2}{\alpha^2}\right)^{-2}$.

Denoting $p = \frac{c}{a} - \frac{b^2}{3a^2} = -\frac{1}{48}$, and $q(\overline{C_\nu}) = \frac{2b^3}{27a^3} - \frac{bc}{3a^2} + \frac{d(r_\nu)}{a} = \frac{-2}{27\cdot 4^3} + \frac{1}{4}\left(32\pi^2\frac{r_\nu^2}{\alpha^2}\right)^{-2} = \frac{1}{4096\pi^4}\frac{\alpha^4}{r_\nu^4} - \frac{1}{864}$ and defining

$$\begin{aligned}\Delta(r_\nu) &= q(r_\nu)^2 + \frac{4p^3}{27} \\ &= \left(\frac{1}{4096\pi^4}\frac{\alpha^4}{r_\nu^4} - \frac{1}{864}\right)^2 - \frac{1}{746\,496}\end{aligned} \tag{38}$$

and by solving this cubic equation we have 3 solutions:

$$x_1(r_\nu) = t(r_\nu) + \frac{1}{12} \tag{39}$$

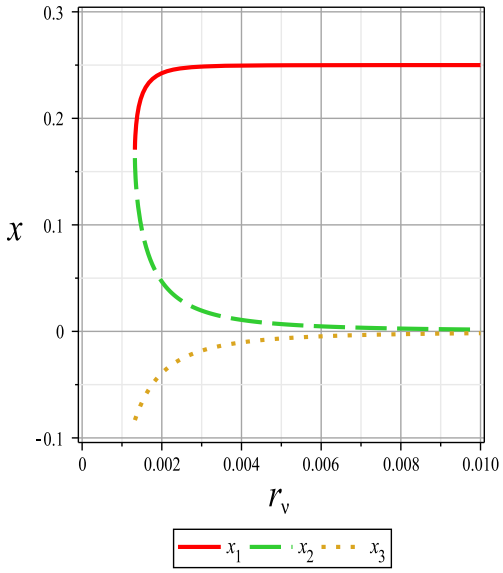

Fig. 4 Three roots of (37) for $x = z^2 = (m_\nu/m_A)^2$.

where $t(r_\nu) = \left(-\frac{q(r_\nu)}{2} + \frac{1}{2}\sqrt{\Delta(r_\nu)}\right)^{1/3} + \left(-\frac{q(r_\nu)}{2} - \frac{1}{2}\sqrt{\Delta(r_\nu)}\right)^{1/3}$,

$$x_2(r_\nu) = -\frac{t(r_\nu)}{2} + \sqrt{\frac{t(r_\nu)^2}{4} + \frac{q(r_\nu)}{t(r_\nu)}} + \frac{1}{12} \tag{40}$$

and

$$x_3(r_\nu) = -\frac{t(r_\nu)}{2} - \sqrt{\frac{t(r_\nu)^2}{4} + \frac{q(r_\nu)}{t(r_\nu)}} + \frac{1}{12} \tag{41}$$

We must observe that only x_1 and x_2 are positive numbers while x_3 is negative, as we observe in Fig. 4 that show x_1 , x_2, and x_3 as function of r_ν.

Both solutions x_1 and x_2 determine two direct relations between the axion mass and the neutrino mass: $m_A = x_1^{-1/2}(r_\nu)m_\nu$ and $m_A = x_2^{-1/2}(r_\nu)m_\nu$. In Fig. 4, we display the two asymptotic cases by considering two situations:

Situation I: $z << 1$;

In this situation, we can consider the approximation: $G(z) = z^2\sqrt{1-4z^2} \approx z^2 - 2z^4 = \frac{\alpha^2}{32\pi^2 r_\nu^2}$, which leads to a simple relation:

$$\frac{m_\nu}{m_A} \approx \frac{\sqrt{1-\sqrt{1-\frac{\alpha^2}{4\pi^2 r_\nu^2}}}}{2} \tag{42}$$

valid for $r_\nu \geq \frac{\sqrt{3\sqrt{3}}\alpha}{4\pi} \simeq 0.00132$, which asymptotically behaves as

$$\frac{m_\nu}{m_A} \sim \frac{1}{4\sqrt{2}}\frac{\alpha}{\pi r_\nu} \tag{43}$$

and therefore $\frac{m_\nu}{m_A} \to 0$ when $r_\nu \to \infty$.

Situation II: $z \approx 1/2$;

In this case, we consider the approximation: $G(z) = z^2\sqrt{1-4z^2} = z^2\sqrt{(1-2z)(1+2z)} \approx \frac{1}{4}\sqrt{2(1-2z)} = \frac{\alpha^2}{32\pi^2 r_\nu^2}$. We have

$$\frac{m_\nu}{m_A} \sim \frac{1}{2} - \frac{\alpha^4}{256\pi^4 r_\nu^4} \to \frac{1}{2} \tag{44}$$

for higher r_ν.

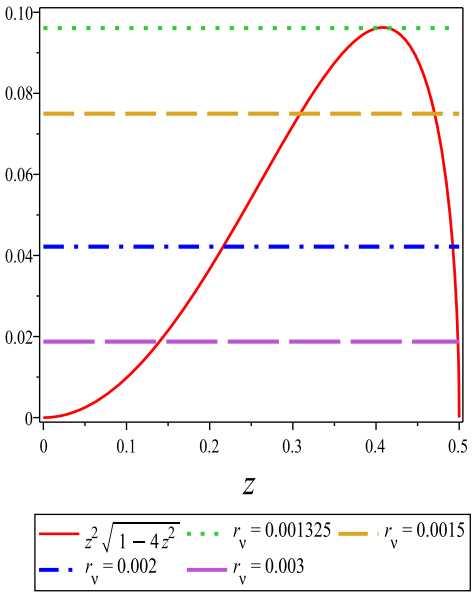

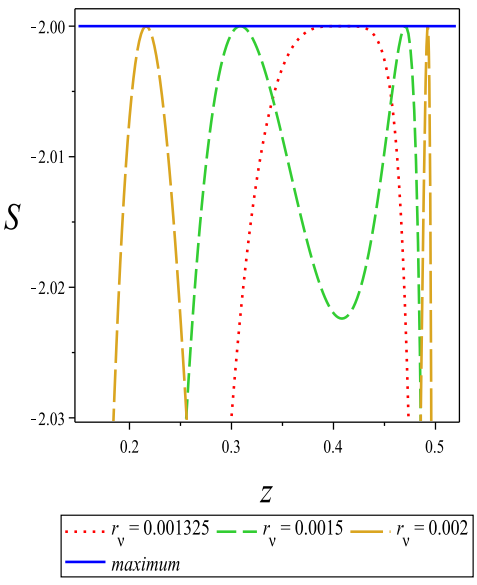

Fig. 5 (*Left plot*) This plot shows the condition to maximum: $BR_0 = 1/2$. The *parallel lines* represent different values of $\left(32\pi^2\frac{r_\nu^2}{\alpha^2}\right)^{-1}$, while the curve corresponds to the plot of $z^2(1-4z^2)$. We can see that given r_ν, we obtain two distinct values of z. (*Right plot*) This plot corresponds to the same situation of the left-top plot looking for the entropy. The maximum $S_0 = -2$ occurs for two different values of z corresponding to the intersection points in the previous figure. It is important to see that for $r_\nu = 0.00132$, corresponds to an unique z which is exactly $1/\sqrt{6} \simeq 0.408$

Let us better explore some important points. In Fig. 5, we can observe this result from two different ways. Left plot shows the maximum condition $BR_0 = 1/2$. The parallel lines represent different values of $\left(32\pi^2 \frac{r_\nu^2}{\alpha^2}\right)^{-1}$ while the curve corresponds to the plot of $z^2(1-4z^2)^{1/2}$. We can see that given r_ν, we obtain two distinct values of z (two intersections). For $r_\nu \simeq 0.00132$, we have a single intersection point which corresponds to the $z = 1/\sqrt{6} \simeq 0.408$. In the right plot, we check the same situation but looking for the entropy. We consider S_0 in the base two and not e. This implicates that the maximum of the S_0 is -2 ($BR_0 = BR_1 = 1/2$). This global maximum occurs for two distinct z-values for different values of r_ν except by $z = 1/\sqrt{6}$ (or $r_\nu = 0.00132$).

References

1. D. d'Enterria. arXiv:1208.1993 [hep-ph]
2. The ATLAS Collaboration, ATLAS-CONF-2016-081
3. A. Alves, A.G. Dias, R. da Silva, Physica **420**, 1 (2014). arXiv:1408.0827 [hep-ph]
4. E.T. Jaynes, Phys. Rev. **106**, 620 (1957)
5. Maximum Entropy and Bayesian Methods, in *Fundamental Theories of Physics Series*, ed. by Fougère P.F., Vol. 39 (Kluwer Academic Publishers, 1989)
6. T.M. Cover, J.A. Thomas, *Elements of Information Theory*, 2nd edn. Wiley-Interscience (2006)
7. C.E. Shannon, Bell Syst. Tech. J. **27**, 379 (1948). [Bell Syst. Tech. J. 27, 623 (1948)]
8. A.E. Bernardini, R. da Rocha, Phys. Lett. B **762**, 107 (2016)
9. R.A.C. Correa, D.M. Dantas, C.A.S. Almeida, R. da Rocha, Phys. Lett. B **755**, 358 (2016)
10. R. Casadio, R. da Rocha, Phys. Lett. B **763**, 434 (2016)
11. A.E. Bernardini, N.R.F. Braga, R. da Rocha, Phys. Lett. B **765**, 81 (2017)
12. M. Gleiser, N. Stamatopoulos, Phys. Lett. B **713**, 304 (2012)
13. M. Gleiser, D. Sowinski, Phys. Lett. B **747**, 125 (2015)
14. R.D. Peccei, H.R. Quinn, Phys. Rev. Lett. **38**, 1440 (1977)
15. S. Weinberg, Phys. Rev. Lett. **40**, 223 (1978)
16. F. Wilczek, Phys. Rev. Lett. **40**, 279 (1978)
17. J.E. Kim, G. Carosi, Rev. Mod. Phys. **82**, 557 (2010). arXiv:0807.3125 [hep-ph]
18. J. Jaeckel, A. Ringwald, Ann. Rev. Nucl. Part. Sci. **60**, 405 (2010). arXiv:1002.0329 [hep-ph]
19. A.G. Dias, A.C.B. Machado, C.C. Nishi, A. Ringwald, P. Vaudrevange, JHEP **1406**, 037 (2014). arXiv:1403.5760 [hep-ph]
20. S.F. King. arXiv:1701.04413 [hep-ph]
21. P.A.R. Ade, et al. (Planck Collaboration), Astron. Astrophys. **594**, A13 (2016). arXiv:1502.01589 [astro-ph.CO]
22. J. Cichon, Z. Golebiewski, 23rd International meeting on probabilistic, combinatorial and asymptotic methods for the analysis of algorithms. http://luc.devroye.org/AofA2012-CfP.html
23. E. Armengaud, et al., JINST **9**, T05002 (2014). arXiv:1401.3233 [physics.ins-det]
24. C. Patrignani, et al. (Particle Data Group), Chin. Phys. C **40**, 100001 (2016)
25. A. Ayala, I. Dominguez, M. Giannotti, A. Mirizzi, O. Straniero, Phys. Rev. Lett. **113**(19), 191302 (2014). arXiv:1406.6053 [astro-ph.SR]
26. N. Viaux, M. Catelan, P.B. Stetson, G. Raffelt, J. Redondo, A.A.R. Valcarce, A. Weiss, Phys. Rev. Lett. **111**, 231301 (2013). arXiv:1311.1669 [astro-ph.SR]
27. S.J. Asztalos, et al. (ADMX Collaboration), Nucl. Instrum. Meth. A **656**, 39 (2011). arXiv:1105.4203 [physics.ins-det]
28. D. Horns, J. Jaeckel, A. Lindner, A. Lobanov, J. Redondo, A. Ringwald, JCAP **1304**, 016 (2013). arXiv:1212.2970 [hep-ph]
29. A. Caldwel, et al. (MADMAX Working Group). arXiv:1611.05865 [physics.ins-det]
30. A.J. Millar, G.G. Raffelt, J. Redondo, F.D. Steffen. arXiv:1612.07057 [hep-ph]
31. P. Petreczky, H.P. Schadler, S. Sharma, Phys. Lett. B **762**, 498 (2016). arXiv:1606.03145 [hep-lat]
32. S. Borsanyi, et al., Nature **539**(7627), 69 (2016). arXiv:1606.07494 [hep-lat]
33. A.R. Zhitnitsky, Sov. J. Nucl. Phys. **31**, 260 (1980). [Yad. Fiz. 31 (1980) 497]
34. M. Dine, W. Fischler, M. Srednicki, Phys. Lett. B **104**, 199 (1981)
35. A. Celis, J. Fuentes-Martin, H. Serodio, Phys. Lett. B **737**, 185 (2014). arXiv:1407.0971 [hep-ph]
36. A. Celis, J. Fuentes-Martin, H. Serodio, Phys. Lett. B **741**, 117 (2015). arXiv:1410.6217 [hep-ph]
37. J.D. Clarke, R.R. Volkas. arXiv:1509.07243 [hep-ph]
38. A.G. Dias, V. Pleitez, Phys. Rev. D **73**, 017701 (2006). [hep-ph/0511104]